Ionization effect in the Earth's atmosphere due to cosmic rays during the GLE # 71 on 17 May 2012

Susanna Pätsi [a], Alexander Mishev [b,c,*]

[a] *Faculty of Science, University of Oulu, Oulu, Finland*
[b] *Sodankylä Geophysical Observatory, University of Oulu, Oulu, Finland*
[c] *Space Physics and Astronomy Research Unit, University of Oulu, Oulu, Finland*

Abstract

Nowadays the systematic study of the possible effect of precipitating high-energy particles on atmospheric physics and chemistry is in great expansion. Most of the recent models studying the precipitating energetic particles effects in the Earth's atmosphere are based on reliable quantification of the induced ionization, that is, the cosmic ray impact ionization, which is extensively studied over the last decade. While the galactic cosmic rays are the main source of ionization in the Earth's stratosphere and troposphere, the energetic particles of solar origin can significantly enhance the ion production following strong solar eruptions, specifically over the polar caps. A particular interest represents solar protons observed by ground-based detectors, viz. the so-called ground level enhancements (GLE), observed as an increase of the count rate of e.g. neutron monitors. Here, employing 3-D Monte Carlo model, we computed the solar protons induced atmospheric ionization during the moderate GLE # 71 on 17 May 2012. The ion production rates were computed during various stages of the event as a function of the altitude above sea level using derived by verified model particles spectra. The 24 h averaged ionization effect relative to the average due to the galactic cosmic rays was computed at several depths in the atmosphere.
© 2022 COSPAR. Published by Elsevier B.V. This is an open access article under the CC BY license (http://creativecommons.org/licenses/by/4.0/).

1. Introduction

The precipitation of high-energy charged particles of extra-terrestrial origin impacts various processes in the Earth's atmosphere, specifically by the induced ionization and the corresponding influence on atmospheric physics and chemistry (e.g. Turunen et al., 2009; Calisto et al., 2011; Rozanov et al., 2012; Mironova et al., 2015; Nilsen et al., 2021, and references therein). Different populations of energetic precipitating particles (EPPs) and/or radiation contribute to the atmospheric ionization, that is,

high-energy solar electromagnetic radiation such as UV, EUV, and X-ray determine the ion production in the upper atmosphere. At the same time, high-energy particles contribute mainly to the stratospheric and tropospheric ionization, that is below circa 100 km above sea level (asl), the atmospheric ionization is predominantly due to the omnipresent slightly variable flux of galactic cosmic rays (GCRs), which secodaries produced in the particle shower induce ionization (for details see the review by Mironova et al., 2015, and references therein). The atmospheric ionization is sporadically enhanced following solar eruptions by the so-called solar energetic particles (SEPs) (e.g. Funke et al., 2011; Jackman et al., 2011; Usoskin et al., 2011b; Mishev and Velinov, 2018). Detailed study of the GCRs/SEPs induced ionization allows one to provide

---

* Corresponding author at: Space Physics and Astronomy Research Unit, University of Oulu, Finland
E-mail address: alexander.mishev@oulu.fi (A. Mishev).

reliable basis to study and/or quantify the impacted by EEPs atmospheric effects (e.g. Usoskin et al., 2009; Mishev et al., 2011; Krivolutsky and Repnev, 2012; Mishev and Velinov, 2018; Riley et al., 2018; Mishev and Velinov, 2020) and the related phenomena (e.g. Bazilevskaya et al., 2008; Vainio et al., 2009; Mironova et al., 2015; Miroshnichenko, 2018, and references therein).

The high-energy GCRs and SEPs, the latter when occur, entering the Earth's atmosphere, initiate particle shower, that is nuclear-electromagnetic-meson cascade yielding large amounts of secondaries, eventually deposing their energy in the atmosphere mostly by ionization of the ambient air (for details see Gaisser et al., 2016). The omnipresent flux of GCRs consists of protons ($\sim$90%) and α-particles ($\sim$8%), yet small amount of heavier nuclei are also observed (Aguilar et al., 2021). The GGRs are modulated in the heliosphere (e.g. Potgieter, 2013, and references therein) and their flux is also influenced by transients and/or other short duration anisotropy of GCR flux not related to the modulation (see e.g. Forbush, 1937; Gil et al., 2018). High-energy SEPs are accelerated during solar eruptive events, such as solar flares and coronal mass ejections (CMEs) (e.g. Desai and Giacalone, 2016; Klein and Dalla, 2017, and references therein) and similarly to GCRs can induce particle shower in the atmosphere, whose secondary particles eventually ionize the ambient air. A specific interest is paid to SEPs whose secondary particles can reach the ground, that is ground level enhancements (GLEs) (e.g. Poluianov et al., 2017). GLEs may considerably enhance the atmospheric ionization specifically over the polar caps (e.g. Jackman et al., 2000; Jackman et al., 2011), thus giving basis to decipher the influence of EEPs on different atmospheric chemistry processes (e.g. Krivolutsky et al., 2006; Randall et al., 2007; Nicoll and Harrison, 2014; Verronen et al., 2015; Sinnhuber et al., 2018).

Since GLEs occur sporadically and naturally differ from each other in spectra and duration (e.g. Moraal and McCracken, 2012; Gopalswamy et al., 2012; Gopalswamy et al., 2014) as well as geomagnetic conditions, they are usually studied on a case-by-case basis (e.g. Miroshnichenko, 2018, and references therein). Besides, different teams derive considerably different SEP spectra, even for the same GLE, resulting on significantly different assessment of CR impact on the atmospheric and/or space weather effects (e.g. Bütikofer and Flückiger, 2013). Here we consider the GLE # 71, occurred on 17 May 2012, using recently derived and verified by direct space-borne measurement SEP spectra (e.g. Mishev et al., 2014; Koldobskiy et al., 2019b; Koldobskiy et al., 2019a; Mishev et al., 2021) and appropriate model described in Section 2.

2. Employed model for computation of cosmic ray induced ionization

The ion production rate in the atmosphere due to GCRs and SEPs can be assessed by analytical or empirical models (e.g. Vitt and Jackman, 1996), yet naturally they reveal limited application to given atmospheric region, cascade component, or primary particle (e.g. Velinov et al., 2013, and references therein). This fact implied the development of more sophisticated models, that is, based on simulations. Over the last two decades several full target models based on Monte Carlo simulations of the cosmic ray induced cascades have been developed, which allowed one to compute the ion production rate in the Earth's atmosphere realistically considering all the physical processes (e.g. Desorgher et al., 2005; Usoskin and Kovaltsov, 2006; Paschalis et al., 2014; Banjac et al., 2019). Here, we employed a model similar to Usoskin and Kovaltsov (2006), the full description given by Velinov et al. (2009).

The ion production rate in $ionpars/s.cm^3$ as a function of the altitude asl is given by:

$$q(h,E) = \frac{1}{E_{ion}} \sum_i \int_{E_{cut}(R_c)}^{\infty} \int_{\Omega} D_i(E) Y(h,E) \rho(h) dE d\Omega \qquad (1)$$

h is the air overburden (air mass) above a given altitude in the atmosphere expressed in g/cm^2 or altitude asl, $D_i(E)$ is the differential cosmic ray spectrum for a given component i: protons p, Helium (α-particles), ρ is the atmospheric density in g/cm^3, which can be expressed using arbitrary models, E is the initial energy of the incoming primary nuclei on the top of the atmosphere, Ω is a solid angle and $E_{ion} = 35$ eV is the average energy necessary to yield an ion pair in air (Porter et al., 1976). Note that the heavier nuclei with atomic number $Z > 2$ of the GCRs are scaled to α-particles according to Usoskin and Kovaltsov (2006), Mishev and Velinov (2011). The integration is over the kinetic energy $E_{cut}(R_c)$ above the rigidity cut-off R_c (Cooke et al., 1991) for a nuclei of type i at a given geographic location by the expression:

$$E_{cut,i} = \sqrt{\left(\frac{Z_i}{A_i}\right)^2 R_c^2 + E_0^2} - E_0 \qquad (2)$$

where $E_0 = 0.938$ GeV/n is the proton's rest mass and the ionization yield function and given altitude h or mass overburden is defined as:

$$Y(h,E) = \frac{\partial E(h,E)}{\partial h} \qquad (3)$$

where ∂E is the deposited energy in an atmospheric layer ∂h. The yield function is the response of the ambient air at a given atmospheric depth as deposited energy (ionization) to a mono-energetic unit flux of primary particle entering into the Earth's atmosphere. The formalism of precomputed yield functions is well known, widely used and easy for application. Once the yield functions been obtained by Monte Carlo simulations, allow one, without subsequent extensive computations, to assess the ion production rate as an integral of the product of the primary particle spectrum and the yield functions. In the model we use yield functions computed with the PLANETOCOSMICS code (for details see Desorgher et al., 2005), which

differs from Usoskin and Kovaltsov (2006),Velinov et al. (2009) in the employed hadron generators (for details see Mishev and Velinov, 2010; Mishev and Velinov, 2014), yet the difference in ion production is about 15–20% (for details see Usoskin et al., 2009), mostly due to the particle shower development (for details see Engel et al., 2011).

Here the rigidity cut-offs over the globe can be computed with the MAGNETOCOSMICS code, explicitly considering the measured K_p index corresponding to the exact period of the GLE occurrence (Desorgher et al., 2005). Routinely, during the computations, a combination of the IGRF geomagnetic model as the internal field (Thébault et al., 2015) and the Tsyganenko 89 model as the external field (Tsyganenko, 1989) were employed allowing straightforward computations (Kudela and Usoskin, 2004; Kudela et al., 2008; Nevalainen et al., 2013). Note, that during GLEs, the atmospheric ionization is a superposition of GCRs and SEPs contributions (e.g. Usoskin et al., 2009; Mishev et al., 2013; Mishev and Velinov, 2015).

A simple one-parameter model allows one to consider with reasonable precision the contribution of GCRs in Eq. (1), that is the force field model (Gleeson and Axford, 1968; Caballero-Lopez and Moraal, 2004), where the parametrization of the local interstellar spectrum is according to Usoskin et al. (2017) and the modulation potential is computed as in Usoskin et al. (2011a). Accordingly, the SEPs spectra in Eq. (1) are taken from Mishev et al. (2021). Note, that for the computations is employed a realistic atmospheric model NRLMSISE-00 (Picone et al., 2002).

3. GLE # 71 and the corresponding ionization effect

GLE # 71 occurred on 17 May 2012, following eruptive processes in the active region NOAA 11476, namely CME and a moderately strong flare (class M5.1) at 01:25 UT. It was registered by the global neutron monitor (NM) network at around 01:50 UT with a moderate increase revealed by APTY, OULU, and SOPO/SOPB (Apatity, Oulu, and South Pole) NMs, while the other NMs registered only marginal count rate increases. The NM count rate increase was observed for about two hours (e.g. Kocharov et al., 2018; Anastasiadis et al., 2019).

3.1. Ion production rate in the atmosphere

Using the model described in Section 2 and the derived SEP spectra by Mishev et al. (2021), depicted in Fig. 1, we computed the ion production rate at several depths (mass overburden) in the atmosphere. Here we considered 5-min SEP spectra (for details see their Table 2 Mishev et al., 2021). Therefore, we computed the ion production rate in the atmosphere with 5-min time resolution considering explicitly the dynamical evolution of the SEP spectra.

An illustration of the computed ion production rate as a superposition of GCRs and SEPs contributions during the peak intensity phase (02:00 UT) of GLE # 71 at depths 100 g cm^{-2} and 200 g cm^{-2} roughly corresponding to the due to GCRs Regener-Pfotzer maximum (Regener and Pfotzer, 1935) is presented in Fig. 2 and Fig. 3, respectively (detailed information is provided in the suppl. material as. csv file). The ion production rate is comparable to that during the peak phase of the third Halloween event, that is GLE # 67 on 2 November 2003 (for details see the supplementary material and Fig. 2 in Mishev and Velinov, 2020), yet the SEP spectra are softer, therefore the altitude of maximum ion production rate during GLE # 71 is greater than the recently studied GLE # 65 and GLE # 67 (for details see Mishev and Velinov, 2020). This is clearly seen by the altitude dependence of the ion production rate due to the GCRs and SEPs during GLE # 71, presented as supplementary material (animation). While the Regener-Pfotzer maximum is clearly seen for the GCRs (suppl. material 1), the SEPs deposit their energy at greater altitudes, that is, at depths of about 10–25 g cm^{-2} as presented in the supplementary materials 2 and 3 (the ion production rate due to the superimposed GCRs and SEPs contributions as a function of the altitude during the event onset and peak phase of the event). Note, that the contribution of the GCRs to the ion production rate is in agreement with widely used and/or recent models for computation of the atmospheric ionization (e.g. Usoskin and Kovaltsov, 2006; Banjac et al., 2019; Makrantoni et al., 2021).

The ion production rate during the GLE # 71 was significant throughout the event onset and peak phase of the event, specifically in the polar stratosphere and troposphere (see Fig. 2, Fig. 3 and the suppl. material). Because of the softer SEP spectra compared to that of GCRs, the ion production rate rapidly diminished, specifically at depths below 200–250 g cm^{-2}. At depths of about 200 g cm^{-2}, the contribution of the GCRs and SEPs are almost equal, whilst below this level the contribution of the former dominated. Besides, the ion production rate due to SEPs govern the atmospheric ionization in a region with rigidity cut-off till of about $R_c \approx 3$ GV, whilst at greater rigidity cut-off the ion production rate was due mainly to GCRs, that is, in the region of $R_c \geqslant 3$ GV, the ion production due to GCRs dominated in the whole atmosphere.

3.2. Averaged ionization effect

For providing reliable basis for quantification of the terrestrial effects of the precipitating high-energy particles in the atmosphere, namely SEPs and GCRs, specifically for the atmospheric physics and chemistry purposes, it is necessary to normalize the ion production. Therefore, we computed the ionization effect over selected time scale e.g. 24 h (Turunen et al., 2009; Mironova et al., 2015).

Here, employing the recombination model by Krivolutsky et al. (2006) and integrating the ion production rates during the GLE # 71 (see subSection 3.1), we
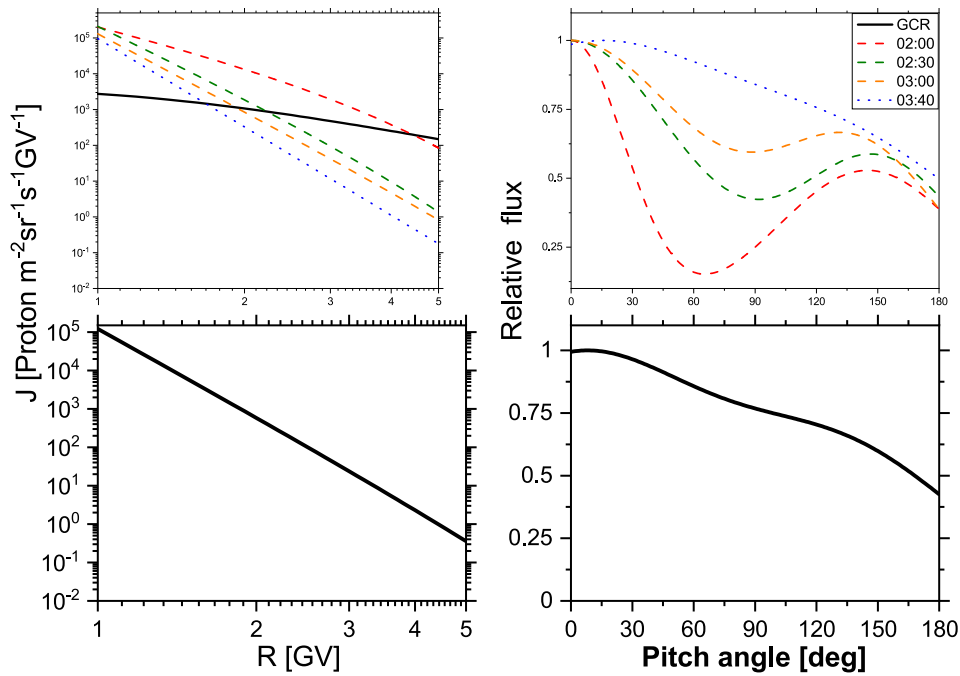
Fig. 1. Top panels: spectra and PAD of SEPs during several stages of GLE # 71 on 17 May 2012 as depicted in the legend. Bottom panels: averaged over the event spectra and PAD of SEPs during GLE # 71.

assessed the 24^h averaged ionization effect in the atmosphere during GLE # 71 at selected atmospheric depths (altitudes). The averaged ionization effect represents the integrated on a step of 5-min ion production during the event considering the actual SEP flux including its time evolution with the GCR contributions versus the averaged

ion production rate due to GCRs before the event on a 24 h time scale.

An example of the ionization effect at an atmospheric depth of 50 g cm^{-2} is shown in Fig. 4. While the 24^h averaged ionization effect is significant at altitudes of about 10–50 g cm^{-2}, it drops at depths of 100 g cm^{-2} and 200 g cm^{-2},
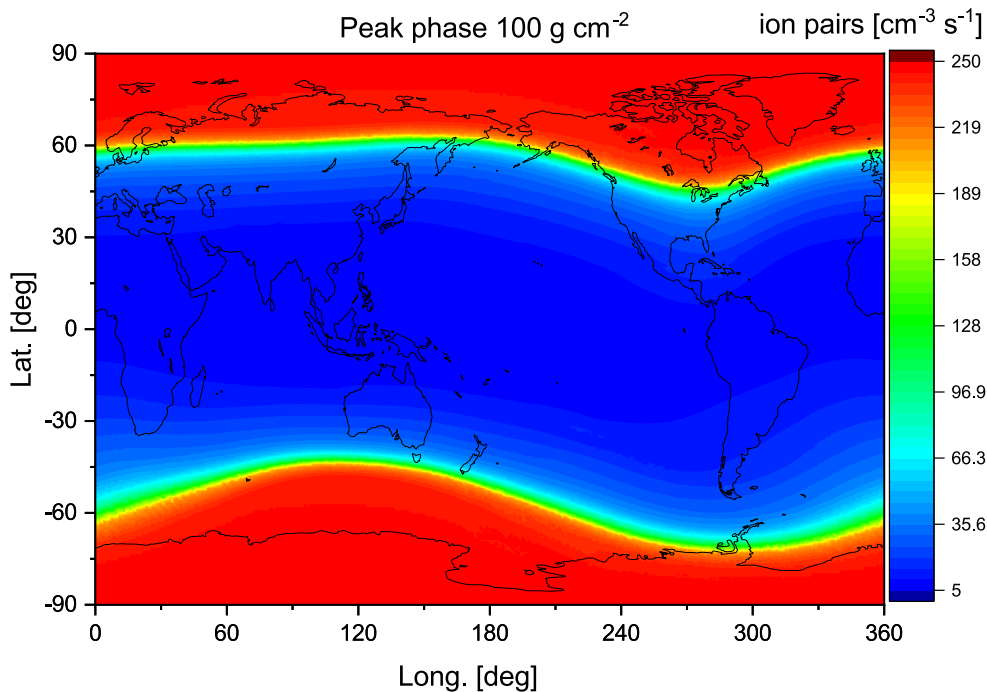

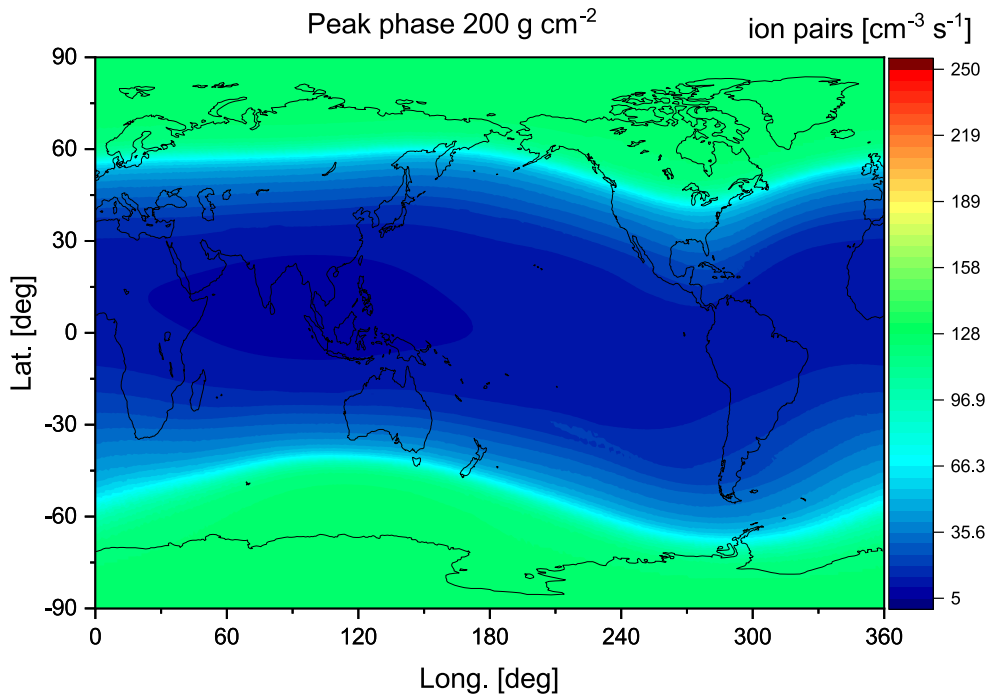Fig. 2. Ion production rate at 100 g cm^{-2} during the peak phase of GLE # 71 on 17 May 2012.

Fig. 3. Ion production rate at 200 g cm^{-2} during the peak phase of GLE # 71 on 17 May 2012.

as depicted in Fig. 5 and Fig. 6, respectively (the details are given in the suppl. material as.csv files). Note, during all the computations of ion production rates, accordingly the ionization effect, the cut-off rigidities were considered taking into account the goemagnetospheric conditions during the event, that is, the computations were performed employing a combination of IGRF and Tsyganenko 89

models, as discussed above. This allowed us to quantify with good precision the ionization effect on a global scale during the GLE # 71.

One can see that the 24 h overaged ionization effect during GLE # 71 ranges from about 90% at depths of 50 g cm^{-2} and drops to $\approx$20% at depths of 200 g cm^{-2}. At lower depths the 24 h ionization effect was marginal.
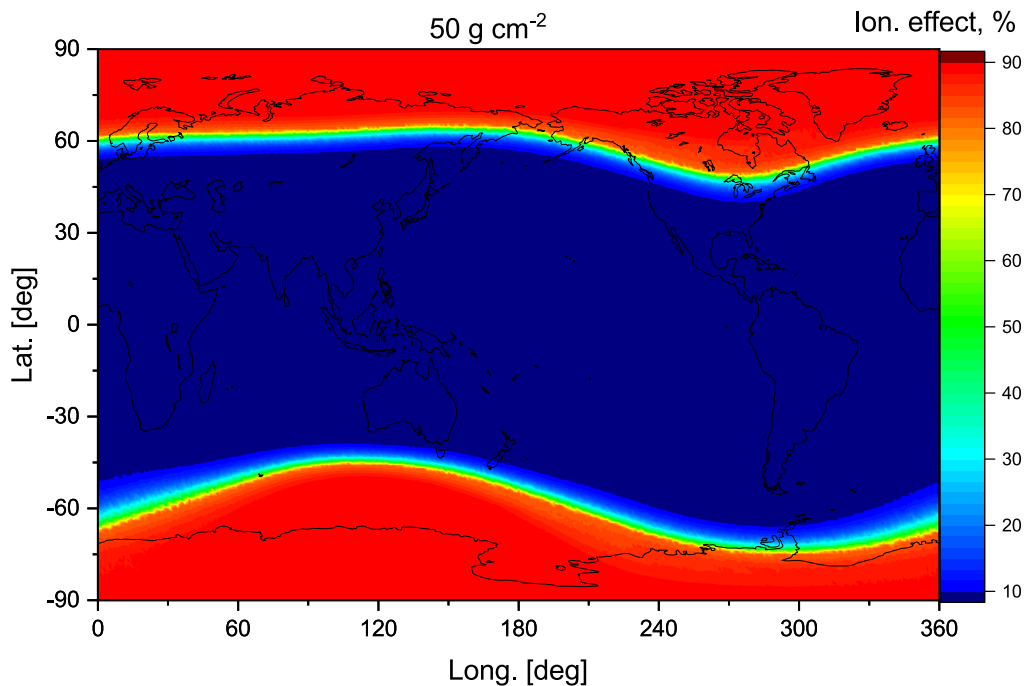

Fig. 4. 24^h averaged ionization effect at 50 g cm^{-2} during GLE # 71 on 17 May 2012.
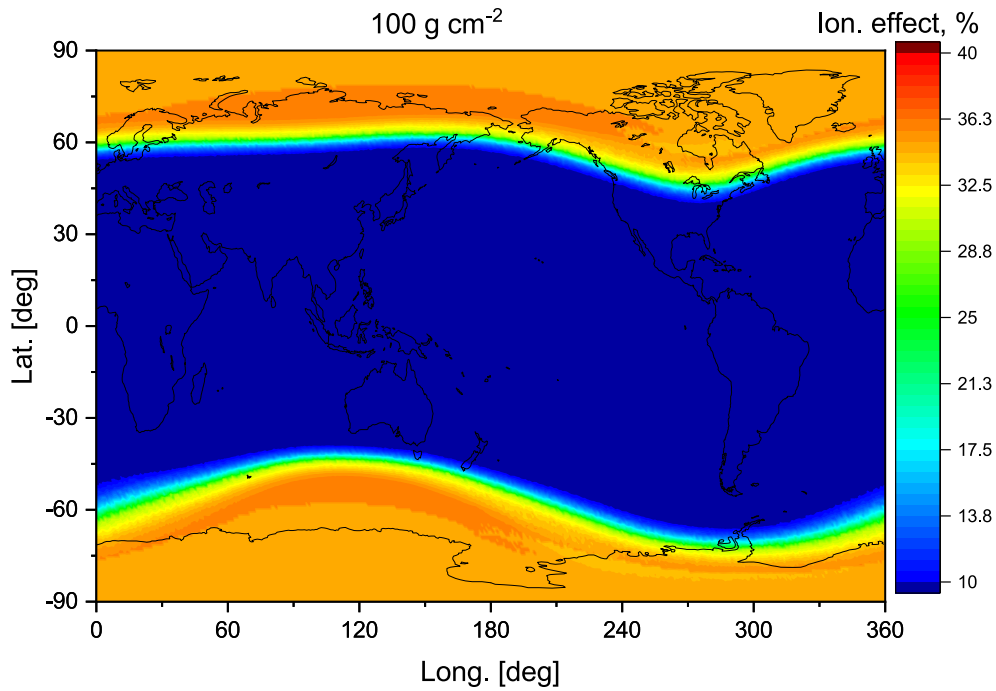
Fig. 5. 24^h averaged ionization effect at 100 g cm^{-2} during GLE # 71 on 17 May 2012.

4. Summary

In this work, we computed the ion production rate and the corresponding ionization effect during the GLE # 71 on 17 May 2012. Here we used high-precision verified SEP spectra including their time evolution throughout the event, and state-of-the-art based on Monte Carlo simulations model, considering explicitly the geomagneto-spheric conditions.

The computed ion production rates were significant during the event onset and peak phase of the event, and diminished during the late phase of the event. The ion production
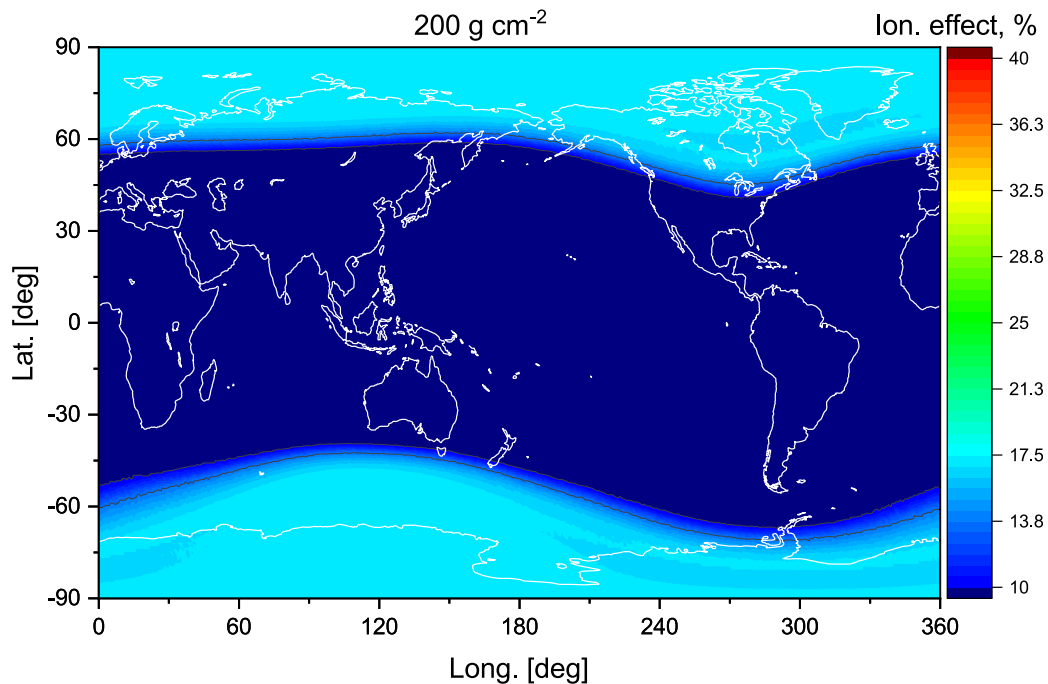

Fig. 6. 24^h averaged ionization effect at 200 g cm^{-2} during GLE # 71 on 17 May 2012.

rates were significant, specifically in the polar stratosphere and polar upper troposphere. At regions with $R_c \approx 2$–3 GV, the ion production was comparable to the average due to GCRs, because of the relatively soft SEP spectra. At mid-latitudes, the ion production due to GCRs dominated in the whole atmosphere. An illustration of the ion production rates and its altitude dependence during the event onset and peak phase was depicted in the supplementary materials (animations and.csv files). The 24^h averaged ionization effect at several depths is also computed and it was shown that it ranged from about 90% at depths of 50 g cm^{-2} to about 20% at depths of 200 g cm^{-2}, respectively.

The presented here study of the ionization effect during a moderately strong GLE, allows one to quantify the possible CR-induced effects in the Earth's atmosphere (e.g. Miroshnichenko, 2018, and references therein).

Declaration of Competing Interest

The authors declare that they have no known competing financial interests or personal relationships that could have appeared to influence the work reported in this paper.

Acknowledgements

Appendix A. Supplementary material

Animation 1: The contribution of GCRs to the ion production rate as function of the altitude during GLE # 71 on 17 May 2012. Animation 2: The superimposed (GCRs and SEPs) ion production rate as function of the altitude during the event onset of GLE # 71 on 17 May 2012. Animation 3: The ion production rate as function of the altitude during the peak phase of GLE # 71 on 17 May 2012. 100gIonRate.csv Global map (column 1 latitude, column 2 longitude) of ion production rate due to GCR protons (column 3) and α-particles (column 4), SEPs (column 5) and superimposed (column 6) at depth of 100 g cm^{-2} during the peak phase of GLE # 71 on 17 May 2012. 200gIonRate.csv Global map (column 1 latitude, column 2 longitude) of ion production rate due to GCR protons (column 3) and α-particles (column 4), SEPs (column 5) and superimposed (column 6) at depth of 200 g cm^{-2} during the peak phase of GLE # 71 on 17 May 2012. IonizationEffect.csv Global map (column 1 latitude, column 2 longitude) of the 24 h averaged ionization effect at depth of 100 g cm^{-2} (column 3) and 200 g cm^{-2} (column 4) during GLE # 71 on 17 May 2012. Supplementary data associated with this article can be found, in the online version, at https://doi.org/10.1016/j.asr.2022.02.008.

References

Aguilar, M., Ali Cavasonza, L., Ambrosi, G., Arruda, L., Attig, N., Barao, F., Barrin, L., Bartoloni, A., Başeğmez-du Pree, S., Bates, J., Battiston, R., Behlmann, M., Beischer, B., Berdugo, J., Bertucci, B., Bindi, V., de Boer, W., Bollweg, K., Borgia, B., Boschini, M., Bourquin, M., Bueno, E., Burger, J., Burger, W., Burmeister, S., Cai, X., Capell, M., Casaus, J., Castellini, G., Cervelli, F., Chang, Y., Chen, G., Chen, H., Chen, Y., Cheng, L., Chou, H., Chouridou, S., Choutko, V., Chung, C., Clark, C., Coignet, G., Consolandi, C., Contin, A., Corti, C., Cui, Z., Dadzie, K., Dai, Y., Delgado, C., Della Torre, S., Demirköz, M., Derome, L., Di Falco, S., Di Felice, V., Díaz, C., Dimiccoli, F., von Doetinchem, P., Dong, F., Donnini, F., Duranti, M., Egorov, A., Eline, A., Feng, J., Fiandrini, E., Fisher, P., Formato, V., Freeman, C., Galaktionov, Y., Gámez, C., García-López, R., Gargiulo, C., Gast, H., Gebauer, I., Gervasi, M., Giovacchini, F., Gómez-Coral, D., Gong, J., Goy, C., Grabski, V., Grandi, D., Graziani, M., Guo, K., Haino, S., Han, K., Hashmani, R., He, Z., Heber, B., Hsieh, T., Hu, J., Huang, Z., Hungerford, W., Incagli, M., Jang, W., Jia, Y., Jinchi, H., Kanishev, K., Khiali, B., Kim, G., Kirn, T., Konyushikhin, M., Kounina, O., Kounine, A., Koutsenko, V., Kuhlman, A., Kulemzin, A., La Vacca, G., Laudi, E., Laurenti, G., Lazzizzera, I., Lebedev, A., Lee, H., Lee, S., Leluc, C., Li, J., Li, M., Li, Q., Li, S., Li, T., Li, Z., Light, C., Lin, C., Lippert, T., Liu, Z., Lu, S., Lu, Y., Luebelsmeyer, K., Luo, J., Lyu, S., Machate, F., Mañá, C., Marín, J., Marquardt, J., Martin, T., Martínez, G., Masi, N., Maurin, D., Menchaca-Rocha, A., Meng, Q., Mo, D., Molero, M., Mott, P., Mussolin, L., Ni, J., Nikonov, N., Nozzoli, F., Oliva, A., Orcinha, M., Palermo, M., Palmonari, F., Paniccia, M., Pashnin, A., Pauluzzi, M., Pensotti, S., Phan, H., Plyaskin, V., Pohl, M., Porter, S., Qi, X., Qin, X., Qu, Z., Quadrani, L., Rancoita, P., Rapin, D., Reina Conde, A., Rosier-Lees, S., Rozhkov, A., Rozza, D., Sagdeev, R., Schael, S., Schmidt, S., Schulz von Dratzig, A., Schwering, G., Seo, E., Shan, B., Shi, J., Siedenburg, T., Solano, C., Song, J., Sonnabend, R., Sun, Q., Sun, Z., Tacconi, M., Tang, X., Tang, Z., Tian, J., Ting, S.C., Ting, S., Tomassetti, N., Torsti, J., Tüysüz, C., Urban, T., Usoskin, I., Vagelli, V., Vainio, R., Valente, E., Valtonen, E., Vázquez Acosta, M., Vecchi, M., Velasco, M., Vialle, J., Wang, L., Wang, N., Wang, Q., Wang, S., Wang, X., Wang, Z., Wei, J., Weng, Z., Wu, H., Xiong, R., Xu, W., Yan, Q., Yang, Y., Yi, H., Yu, Y., Yu, Z., Zannoni, M., Zhang, C., Zhang, F., Zhang, F., Zhang, J., Zhang, Z., Zhao, F., Zheng, Z., Zhuang, H., Zhukov, V., Zichichi, A., Zimmermann, N., Zuccon, P., 2021. The Alpha Magnetic Spectrometer (AMS) on the international space station: Part II "Results from the first seven years. Phys. Rep. 894, 1–116. https://doi.org/10.1016/j.physrep.2020.09.003.

Anastasiadis, A., Lario, D., Papaioannou, A., Kouloumvakos, A., Vourlidas, A., 2019. Solar energetic particles in the inner heliosphere: Status and open questions. Philos. Trans. Roy. Soc. A Math. Phys. Eng. Sci. 377. https://doi.org/10.1098/rsta.2018.0100, 20180100.

Banjac, S., Herbst, K., Heber, B., 2019. The atmospheric radiation interaction simulator (atris): Description and validation. J. Geophys. Res. Space Phys. 124, 50–67. https://doi.org/10.1029/2018JA026042.

Bazilevskaya, G.A., Usoskin, I.G., Flückiger, E., Harrison, R., Desorgher, L., Bütikofer, B., Krainev, M., Makhmutov, V., Stozhkov, Y., Svirzhevskaya, A., Svirzhevsky, N., Kovaltsov, G., 2008. Cosmic ray induced ion production in the atmosphere. Space Sci. Rev. 137, 149–173.

Bütikofer, R., Flückiger, E., 2013. Differences in published characteristics of GLE 60 and their consequences on computed radiation dose rates along selected flight paths. J. Phys: Conf. Ser. 409, 012166.

Caballero-Lopez, R., Moraal, H., 2004. Limitations of the force field equation to describe cosmic ray modulation. J. Geophys. Res. 109, A01101.

Calisto, M., Usoskin, I., Rozanov, E., Peter, T., 2011. Influence of galactic cosmic rays on atmospheric composition and dynamics. Atmos. Chem. Phys. 11, 4547–4556.

Cooke, D., Humble, J., Shea, M., Smart, D., Lund, N., Rasmussen, I., Byrnak, B., Goret, P., Petrou, N., 1991. On cosmic-ray cutoff terminology. Il Nuovo Cimento C 14, 213–234.

Desai, M., Giacalone, J., 2016. Large gradual solar energetic particle events. Living Rev. Sol. Phys. 13, 3. https://doi.org/10.1007/s41116-016-0002-5.

Desorgher, L., Flückiger, E., Gurtner, M., Moser, M., Bütikofer, R., 2005. A geant 4 code for computing the interaction of cosmic rays with the earth's atmosphere. Int. J. Mod. Phys. A 20, 6802–6804.

Engel, R., Heck, D., Pierog, T., 2011. Extensive air showers and hadronic interactions at high energies. Ann. Rev. Nucl. Particle Sci. 61.

Forbush, S., 1937. On the effects in cosmic-ray intensity observed during the recent magnetic storm. Phys. Rev. 51, 1108–1109.

Funke, B., Baumgaertner, A., Calisto, M., Egorova, T., Jackman, C., Kieser, J., Krivolutsky, A., López-Puertas, M., Marsh, D., Reddmann, T., Rozanov, E., SalmiS, -M., Sinnhuber, M., Stiller, G., Verronen, P., Versick, S., Von Clarmann, T., Vyushkova, T., Wieters, N., Wissing, J., 2011. Composition changes after the Halloween solar proton event: The high energy particle precipitation in the atmosphere (HEPPA) model versus MIPAS data intercomparison study. Atmos. Chem. Phys. 11, 9089–9139. https://doi.org/10.5194/acp-11-9089-2011.

Gaisser, T., Engel, R., Resconi, E., 2016. Cosmic Rays and Particle Physics. Cambridge University Press, Cambridge, UK.

Gil, A., Kovaltsov, G.A., Mikhailov, V., Mishev, A., Poluianov, S., Usoskin, I., 2018. An anisotropic cosmic-ray enhancement eventon 07-june-2015: A possible origin. Sol. Phys. 293, 154.

Gleeson, L., Axford, W., 1968. Solar modulation of galactic cosmic rays. Astrophys. J. 154, 1011–1026.

Gopalswamy, N., Xie, H., Akiyama, S., Mäkelä, P., Yashiro, S., 2014. Major solar eruptions and high-energy particle events during solar cycle 24. Earth Planets Space 66, 104. https://doi.org/10.1186/1880-5981-66-104.

Gopalswamy, N., Xie, H., Yashiro, S., Akiyama, S., Mäkelä, P., Usoskin, I., 2012. Properties of ground level enhancement events and the associated solar eruptions during solar cycle 23. Space Sci. Rev. 171, 23–60.

Jackman, C., Fleming, E., Vitt, F., 2000. Influence of extremely large solar proton events in a changing stratosphere. J. Geophys. Res. Atmos. 105, 11659–11670.

Jackman, C., Marsh, D., Vitt, F., Roble, R., Randall, C., Bernath, P., Funke, B., López-Puertas, M., Versick, S., Stiller, G., Tylka, A., Fleming, E., 2011. Northern hemisphere atmospheric influence of the solar proton events and ground level enhancement in january 2005. Atmos. Chem. Phys. 11, 6153–6166.

Klein, K.L., Dalla, S., 2017. Acceleration and propagation of solar energetic particles. Space Sci. Rev. 212, 1107–1136. https://doi.org/10.1007/s11214-017-0382-4.

Kocharov, L., Pohjolainen, S., Reiner, M., Mishev, A., Wang, H., Usoskin, I., Vainio, R., 2018. Spatial organization of seven extreme solar energetic particle events. Astrophys. J. Lett. 862. https://doi.org/10.3847/2041-8213/aad18d.

Koldobskiy, S., Bindi, V., Corti, C., Kovaltsov, G., Usoskin, I., 2019a. Validation of the neutron monitor yield function using data from AMS-02 experiment, 2011–2017. J. Geophys. Res. Space Phys. 124, 2367–2379. https://doi.org/10.1029/2018JA026340.

Koldobskiy, S., Kovaltsov, G., Mishev, A., Usoskin, I., 2019b. New method of assessment of the integral fluence of solar energetic (> 1 GV rigidity) particles from neutron monitor data. Sol. Phys. 294. https://doi.org/10.1007/s11207-019-1485-8.

Krivolutsky, A., Klyuchnikova, A., Zakharov, G., Vyushkova, T., Kuminov, A., 2006. Dynamical response of the middle atmosphere to solar proton event of July 2000: Three-dimensional model simulations. Adv. Space Res. 37, 1602–1613. https://doi.org/10.1016/j.asr.2005.05.115.

Krivolutsky, A., Repnev, A., 2012. Impact of space energetic particles on the earth's atmosphere (a review). Geomag. Aeron. 52, 685–716.

Kudela, K., Bučík, R., Bobik, P., 2008. On transmissivity of low energy cosmic rays in disturbed magnetosphere. Adv. Space Res. 42, 1300–1306.

Kudela, K., Usoskin, I., 2004. On magnetospheric transmissivity of cosmic rays. Czech J. Phys. 54, 239–254.

Makrantoni, P., Mavromichalaki, H., Paschalis, P., 2021. Solar cycle variation of the ionization by cosmic rays in the atmosphere at the mid-latitude region of Athens. Astrophys. Space Sci. 366, 70. https://doi.org/10.1007/s10509-021-03978-8.

Mironova, I., Aplin, K., Arnold, F., Bazilevskaya, G., Harrison, R., Krivolutsky, A., Nicoll, K., Rozanov, E., Turunen, E., Usoskin, I., 2015. Energetic particle influence on the earth's atmosphere. Space Sci. Rev. 96.

Miroshnichenko, L., 2018. Retrospective analysis of gles and estimates of radiation risks. J. Space Weather Space Climate 8, A52. https://doi.org/10.1051/swsc/2018042.

Mishev, A., Kocharov, L., Usoskin, I., 2014. Analysis of the ground level enhancement on 17 May 2012 using data from the global neutron monitor network. J. Geophys. Res. 119, 670–679.

Mishev, A., Koldobskiy, S., Usoskin, I., Kocharov, L., Kovaltsov, G., 2021. Application of the verified neutron monitor yield function for an extended analysis of the GLE # 71 on 17 May 2012. Space Weather 19. https://doi.org/10.1029/2020SW002626, e2020SW002626.

Mishev, A., Velinov, P., 2010. The effect of model assumptions on computations of cosmic ray induced ionization in the atmosphere. J. Atmos. Solar Terr. Phys. 72, 476–481.

Mishev, A., Velinov, P., 2011. Normalized ionization yield function for various nuclei obtained with full Monte Carlo simulations. Adv. Space Res. 48, 19–24.

Mishev, A., Velinov, P., 2014. Influence of hadron and atmospheric models on computation of cosmic ray ionization in the atmosphere-extension to heavy nuclei. J. Atmos. Solar Terr. Phys. 120, 111–120.

Mishev, A., Velinov, P., 2015. Time evolution of ionization effect due to cosmic rays in terrestrial atmosphere during GLE 70. J. Atmos. Solar Terr. Phys. 129, 78–86.

Mishev, A., Velinov, P., 2018. Ion production and ionization effect in the atmosphere during the Bastille day GLE 59 due to high energy SEPs. Adv. Space Res. 61, 316–325. https://doi.org/10.1016/j.asr.2017.10.023.

Mishev, A., Velinov, P., 2020. Ionization effect in the earth's atmosphere during the sequence of October-November 2003 Halloween gle events. J. Atmos. Solar Terr. Phys. 211, 105484. https://doi.org/10.1016/j.jastp.2020.105484.

Mishev, A., Velinov, P., Mateev, L., Tassev, Y., 2011. Ionization effect of solar protons in the earth atmosphere - case study of the 20 January 2005 sep event. Adv. Space Res. 48, 1232–1237.

Mishev, A., Velinov, P., Mateev, L., Tassev, Y., 2013. Ionization effect of nuclei with solar and galactic origin in the earth atmosphere during gle 69 on 20 January 2005. J. Atmos. Solar Terr. Phys. 89, 1–7.

Moraal, H., McCracken, K., 2012. The time structure of ground level enhancements in solar cycle 23. Space Sci. Rev. 171, 85–95.

Nevalainen, J., Usoskin, I., Mishev, A., 2013. Eccentric dipole approximation of the geomagnetic field: Application to cosmic ray computations. Adv. Space Res. 52, 22–29.

Nicoll, K., Harrison, R., 2014. Detection of lower tropospheric responses to solar energetic particles at midlatitudes. Phys. Rev. Lett. 112, 225001.

Nilsen, K., Kero, A., Verronen, P., Szelag, M., Kalakoski, N., Jia, J., 2021. Sensitivity of middle atmospheric ozone to solar proton events: A comparison between a climate model and satellites. J. Geophys. Res. Atmos. 126. https://doi.org/10.1029/2021JD034549, e2021JD034549.

Paschalis, P., Mavromichalaki, H., Dorman, L., Plainaki, C., Tsirigkas, D., 2014. Geant4 software application for the simulation of cosmic ray showers in the earth's atmosphere. New Astron. 33, 26–37. https://doi.org/10.1016/j.newast.2014.04.009.

Picone, J., Hedin, A., Drob, D., Aikin, A., 2002. Nrlmsise-00 empirical model of the atmosphere: Statistical comparisons and scientific issues. J. Geophys. Res. Space Phys. 107, 1468.

Poluianov, S., Usoskin, I., Mishev, A., Shea, M., Smart, D., 2017. GLE and sub-GLE redefinition in the light of high-altitude polar neutron monitors. Sol. Phys. 292, 176. https://doi.org/10.1007/s11207-017-1202-4.

Porter, H., Jackman, C., Green, A., 1976. Efficiencies for production of atomic nitrogen and oxygen by relativistic proton impact in air. J. Chem. Phys. 65, 154–167.

Potgieter, M., 2013. Solar Modulation of Cosmic Rays. Living Rev. Sol. Phys. 10, 3. https://doi.org/10.12942/lrsp-2013-3, URL http://link.springer.com/10.12942/lrsp-2013-3.

Randall, C., Harvey, V., Singleton, C., Bailey, S., Bernath, P., Codrescu, M., Nakajima, H., Russell, J., 2007. Energetic particle precipitation effects on the southern hemisphere stratosphere in 1992–2005. J. Geophys. Res. Atmos. 112, D08308.

Regener, E., Pfotzer, G., 1935. Vertical intensity of cosmic rays by threefold coincidences in the stratosphere. Nature 136, 718–719.

Riley, P., Baker, D., Liu, Y., Verronen, P., Singer, H., Güdel, M., 2018. Extreme space weather events: From cradle to grave. Space Sci. Rev. 214, 21. https://doi.org/10.1007/s11214-017-0456-3.

Rozanov, E., Calisto, M., Egorova, T., Peter, T., Schmutz, W., 2012. Influence of the precipitating energetic particles on atmospheric chemistry and climate. Surv. Geophys. 33, 483–501.

Sinnhuber, M., Berger, U., Funke, B., Nieder, H., Reddmann, T., Stiller, G., Versick, S., Von Clarmann, T., Wissing, J., 2018. Noy production, ozone loss and changes in net radiative heating due to energetic particle precipitation in 2002–2010. Atmos. Chem. Phys. 18, 1115–1147. https://doi.org/10.5194/acp-18-1115-2018.

Thébault, E., Finlay, C.C., Beggan, C.D., Alken, P., Aubert, J., Barrois, O., Bertrand, F., Bondar, T., Boness, A., Brocco, L., Canet, E., Chambodut, A., Chulliat, A., Coïsson, P., Civet, F., Du, A., Fournier, A., Fratter, I., Gillet, N., Hamilton, B., Hamoudi, M., Hulot, G., Jager, T., Korte, M., Kuang, W., Lalanne, X., Langlais, B., Léger, J.M., Lesur, V., Lowes, F.J., Macmillan, S., Mandea, M., Manoj, C., Maus, S., Olsen, N., Petrov, V., Ridley, V., Rother, M., Sabaka, T.J., Saturnino, D., Schachtschneider, R., Sirol, O., Tangborn, A., Thomson, A., Tøffner-Clausen, L., Vigneron, P., Wardinski, I., Zvereva, T., 2015. International geomagnetic reference field: the 12th generation. Earth Planets Space 67, 79. https://doi.org/10.1186/s40623-015-0228-9.

Tsyganenko, N., 1989. A magnetospheric magnetic field model with a warped tail current sheet. Planet. Space Sci. 37, 5–20.

Turunen, E., Verronen, P., Seppälä, A., Rodger, C., Clilverd, M., Tamminen, J., Enell, C.F., Ulich, T., 2009. Impact of different energies of precipitating particles on nox generation in the middle and upper atmosphere during geomagnetic storms. J. Atmos. Solar Terr. Phys. 71, 1176–1189.

Usoskin, I., Bazilevskaya, G., Kovaltsov, G., 2011a. Solar modulation parameter for cosmic rays since 1936 reconstructed from ground-based neutron monitors and ionization chambers. J. Geophys. Res. 116, A02104.

Usoskin, I., Gil, A., Kovaltsov, G., Mishev, A., Mikhailov, V., 2017. Heliospheric modulation of cosmic rays during the neutron monitor era: Calibration usingpamela data for 2006–2010. J. Geophys. Res. 122, 3875–3887.

Usoskin, I., Kovaltsov, G., 2006. Cosmic ray induced ionization in the atmosphere: Full modeling and practical applications. J. Geophys. Res., 111

Usoskin, I., Kovaltsov, G., Mironova, I., Tylka, A., Dietrich, W., 2011b. Ionization effect of solar particle gle events in low and middle atmosphere. Atmos. Chem. Phys. 11, 1979–1988.

Usoskin, I.G., Desorgher, L., Velinov, P., Storini, M., Flückiger, E., Bütikofer, R., Kovaltsov, G., 2009. Ionization of the earth's atmosphere by solar and galactic cosmic rays. Acta Geophys. 57, 88–101.

Vainio, R., Desorgher, L., Heynderickx, D., Storini, M., Flückiger, E., Horne, R., Kovaltsov, G., Kudela, K., Laurenza, M., McKenna-Lawlor, S., Rothkaehl, H., Usoskin, I., 2009. Dynamics of the earth's particle radiation environment. Space Sci. Rev. 147, 187–231.

Velinov, P., Asenovski, S., Kudela, K., Lastovička, J., Mateev, L., Mishev, A., Tonev, P., 2013. Impact of cosmic rays and solar energetic particles on the earth's ionosphere and atmosphere. J. Space Weather Space Climate 3, A14.

Velinov, P., Mishev, A., Mateev, L., 2009. Model for induced ionization by galactic cosmic rays in the earth atmosphere and ionosphere. Adv. Space Res. 44, 1002–1007.

Verronen, P., Andersson, M., Kero, A., Enell, C.F., Wissing, J., Talaat, E., Kauristie, K., Palmroth, M., Sarris, T., Armandillo, E., 2015. Contribution of proton and electron precipitation to the observed electron concentration in october-november 2003 and september 2005. Ann. Geophys. 33, 381–394.

Vitt, F., Jackman, C., 1996. A comparison of sources of odd nitrogen production from 1974 through 1993 in the earth's middle atmosphere as calculated using a two-dimensional model. J. Geophys. Res. Atmos. 101, 6729–6739.